

Persistent enhancement of hippocampal network connectivity by parietal rTMS is reproducible

<https://doi.org/10.1523/ENEURO.0129-19.2019>

Cite as: eNeuro 2019; 10.1523/ENEURO.0129-19.2019

Received: 30 March 2019

Revised: 13 September 2019

Accepted: 17 September 2019

This Early Release article has been peer-reviewed and accepted, but has not been through the composition and copyediting processes. The final version may differ slightly in style or formatting and will contain links to any extended data.

Alerts: Sign up at www.eneuro.org/alerts to receive customized email alerts when the fully formatted version of this article is published.

Copyright © 2019 Freedberg et al.

This is an open-access article distributed under the terms of the Creative Commons Attribution 4.0 International license, which permits unrestricted use, distribution and reproduction in any medium provided that the original work is properly attributed.

Title: Persistent enhancement of hippocampal network connectivity by parietal rTMS is reproducible

Abbreviated title: rTMS reproducibility

Authors:

*Michael Freedberg, Ph.D.^{1,2} michael.freedberg@nih.gov
 Jack A. Reeves, B.Ch.E.¹ jack.reeves@nih.gov
 Andrew C. Toader, B.S.¹ actoader@gmail.com
 Molly S. Hermiller, MPPA.³ molly.hermiller@northwestern.edu
 Joel L. Voss, Ph.D.³ joel-voss@northwestern.edu
 Eric M. Wassermann, M.D.¹ wassermanne@ninds.nih.gov
 * Corresponding Author

Affiliations:

1. National Institute of Neurological Disorders and Stroke, Bethesda, MD, 20892, USA
 2. Henry M. Jackson Foundation for the Advancement of Military Medicine, Bethesda, MD, 20817, USA
 3. Northwestern University, Chicago, IL, 60611, USA

Author Contributions: EW, JV and MF Designed Research. MF, JR, and AT Performed Research. MF and MH analyzed the data. All authors contributed to the manuscript.

Corresponding author information: Michael Freedberg, 10 Center Drive, Rm. 7SW 7-5659, Bethesda, MD, 20892, 718-290-6729, michael.freedberg@nih.gov

Number of Figures: 8

Number of Tables: 1

Number of Multimedia: 0

Number of words for Abstract: 248

Number of words for Significant Statement: 98

Number of words for Introduction: 370

Number of words for Discussion: 1,000

Acknowledgements: This work was funded by the Department of Defense in the Center for Neuroscience and Regenerative Medicine. This research was supported (in part) by the Intramural Research Program of the NIH, NINDS

Conflict of Interest: Authors report no conflict of interest.

Funding: This work was funded by the Clinical Neurosciences Program of the National Institute of Neurological Disorders and Stroke and the Center for Neuroscience and Regenerative Medicine (CNRM-70-3904). JV and MH are supported by grants from the National Institutes of Mental Health (R01MH106512) and Neurological Disorders and Stroke (T32NS047987).

Abstract

1
2 Wang et al. (*Science*, 2014: 345, p. 1054) found that that five daily sessions of repetitive
3 transcranial magnetic stimulation (rTMS) of the posterior parietal cortex (PPC) significantly
4 increased functional connectivity (FC) in a network centered on the hippocampus, and caused a
5 correlated increase in memory performance in humans. However, this finding has not been
6 reproduced independently and the requirement for five sessions has not been validated. We
7 aimed to reproduce the imaging results of this experiment, focusing on hippocampal FC
8 changes and using fewer days of rTMS. We measured resting state FC before and after three
9 (N = 9) or four (N = 6) consecutive daily PPC rTMS sessions, using similar delivery parameter
10 settings as Wang et al. Eight subjects received three days of rTMS delivered to the vertex as a
11 control. We employed whole-brain and hypothesis-based statistical approaches to test for
12 hippocampal FC changes. Additionally, we calculated FC in 17 brain networks to determine
13 whether the topographic pattern of FC change was similar between studies. We did not include
14 behavioral testing in this study. PPC, but not vertex, rTMS caused significant changes in
15 hippocampal FC to the same regions as in the previous study. Brain-wide changes in
16 hippocampal FC significantly exceeded changes in global connectedness, indicating that the
17 effect of PPC rTMS was specific to the hippocampal network. Baseline hippocampal FC
18 measured before receiving stimulation predicted the degree of rTMS-induced hippocampal FC
19 increase, as was the case in the previous study. These findings reproduce the imaging findings
20 of Wang et al. and show that FC enhancement can occur after only 3-4 sessions of PPC rTMS.

Significance Statement

21
22 One of the most striking recent findings in the area of neuromodulation is that of Wang et al.
23 (*Science*, 2014: 345, p. 1054), who reported that posterior parietal cortex (PPC) stimulation
24 increased functional connectivity in a network related to declarative memory and centered on
25 the hippocampus, a result with great potential experimental and clinical utility. We used a similar
26 paradigm, with shorter treatment duration and reproduced the effects on connectivity, including
27 specificity for the hippocampal network and dependence on the magnitude of baseline
28 hippocampal connectivity. These results confirm and extend the initial finding and validate the
29 technical approach.

Introduction

Enhancing memory in patients and healthy individuals is a potential application of repetitive transcranial magnetic stimulation (rTMS). Network connectivity modulation with non-invasive brain stimulation has been studied mostly in motor and procedural learning networks (Baraduc et al., 2004; Hotermans et al., 2008; Iezzi et al., 2010; Muellbacher et al., 2002; Rosenthal et al., 2009; Teo et al., 2011; Wilkinson et al., 2015, 2010) and the effects have not been shown to last longer than minutes or hours (Thut and Pascual-leone, 2010). The declarative memory system, on the other hand, has been less explored with rTMS, despite the fact that declarative memory deficits are among the most common and debilitating problems in neurology (Nestor et al., 2005; Vakil, 2005). Wang et al. (2014) increased declarative memory and resting hippocampal network functional connectivity (FC) by delivering multiple-session rTMS to individualized targets in the posterior parietal cortex (PPC), which is connected with the hippocampus via the retrosplenial and parahippocampal cortices (Cavada and Goldman-Rakic, 1989; Mesulam et al., 1977). The FC increase and memory improvement persisted for 24 hours after the final rTMS session and, with reduced strength, for up to approximately two weeks (Wang et al., 2014; Wang and Voss, 2015).

The Wang et al. (2014) findings are a dramatic demonstration of physiological engagement of a specific brain target with correlated behavioral improvement, and are, in this respect, unique in the noninvasive neuromodulation field. However, concern has grown over the rate of false positives in functional neuroimaging (Poldrack et al., 2017) and noninvasive neuromodulation (Héroux et al., 2015; Nahas et al., 2008), resulting in calls for reproduction of results. For example, Héroux et al. (Héroux et al., 2015) found that only between 45 and 60% of experienced researchers were able to reproduce a rTMS effect.

In this study, we used a similar paradigm to that of Wang et al. (2014), with identical targeting procedures and stimulation parameter values, but with fewer stimulation sessions, and without memory testing. We also preprocessed the data somewhat differently, and used vertex

56 stimulation, instead of subthreshold or motor stimulation, as our control condition. Although the
57 original researchers collaborated on this study and shared unpublished data and techniques
58 with us, all data collection, implementation, and analysis were performed independently.

59

60

Methods

Subjects

Twenty-three healthy adults (9 female; age = 19-31 years), free of neurological or psychiatric disorders or medications acting on the central nervous system, participated in the study. Fifteen received active rTMS delivered to the PPC and eight underwent a control procedure with identical stimulation applied to the vertex. All subjects reported being right-handed and passed screening for contraindications to TMS (Rossi et al., 2009) and MRI. Written informed consent was obtained and the study was approved by the local Institutional Review Board.

Procedures

All subjects underwent, in order, baseline scanning, 3 or 4 consecutive daily rTMS sessions, and a post-rTMS scan. Baseline scanning included an anatomical localizer, structural scan (for functional scan co-localization with anatomy, and neuro-navigation), a single resting state scan, and diffusion tensor imaging (not reported here). Nine subjects received three consecutive daily sessions of rTMS delivered to the PPC, six received four daily PPC sessions, and eight received three daily sessions of identical rTMS delivered to the vertex (see “rTMS” section below). The interval between rTMS sessions was approximately 24 hours.

Twelve of our PPC subjects participated in a separate study to find the minimum number of days required to produce a conservative criterion change in hippocampal FC. We found no measurable difference in response between subjects receiving three and four days of rTMS ($W = 36$, $p = 0.327$, 95% CI (-0.074333 0.210993)), so all were included here. The number of stimulation sessions in this study differed from Wang et al. (2014), who delivered stimulation on 5 consecutive days.

Unlike Wang et al. (2014), we used rTMS at the vertex, which produces auditory and somatosensory stimulation, but no significant changes in FC (Jung et al., 2016), as our control condition (see discussion). Subjects underwent the first rTMS session within 36 hours of

87 baseline scanning. The second MRI session occurred on the day after the final rTMS session
88 and within three hours of the time of day of the first scanning session. Subjects were blind to the
89 specific intent of the study and the stimulation condition.

90

91 *fMRI acquisition and preprocessing*

92 MRI was performed on a Siemen's Magnetom 3T scanner using a 16-channel head coil with
93 foam padding to prevent head movement. Subjects were fitted with earplugs and supplied with
94 headphones to protect hearing. During resting scans, subjects were instructed to lie still with
95 their eyes open.

96 Blood oxygen level-dependent (BOLD) data were recorded with a T2*-weighted
97 gradient-echoplanar imaging sequence (EPI: TR = 2,000 ms, TE = 27ms, flip angle = 90°, 36
98 transversal contiguous interleaved slices per volume, 3.0 slice thickness, FOV 22 x 22 cm,
99 matrix size 64 x 64, Voxel size = 3.4 mm x 3.4 mm x 3.0 mm; scan length ~ 6.8 minutes). We
100 acquired structural images with a magnetization-prepared rapid gradient echo sequence
101 (MPRAGE; TR = 2,530 ms, TE = 3.03 ms, 176 slices per volume, 1 mm thickness,
102 FOV = 25.6 × 25.6 cm², 256 × 256 acquisition matrix, Voxel size = 1.0 mm isotropic, 206
103 volumes, 6.83 minutes).

104 We processed the images with Analysis of Functional Images (AFNI; Cox, 1996;
105 RRID:SCR_005927) software. The first five volumes of 206 were removed to ensure that
106 magnetization was stabilized. Preprocessing included motion correction, slice-timing correction
107 to the first slice, functional/structural affine co-registration to Talairach space (TT_N27;
108 Talairach and Tournoux, 1988), resampling to 2.0 mm isotropic voxel resolution, spatial
109 smoothing using a 4 mm full width half maximum (FWHM) Gaussian kernel, and linear
110 detrending. We then scaled each voxel time series to a mean of 100, with a range of 0-200 and
111 regressed head motion from each voxel time series using the mean and derivatives of 6
112 parameter estimates (pitch, roll, yaw, and rotation around each axis). Unlike Wang et al. (2014),

we did not bandpass filter our data because test-retest reliability increases as the highpass cutoff is raised, and even eliminated (Shirer et al., 2015). However, we achieved a high-pass filter via linear detrending using a 2nd or 3rd order polynomial, depending on the subject. We used spatial smoothing, which was omitted by Wang et al. (2014). Finally, frames which included movement displacement greater than 0.3 mm were censored prior to statistical analysis to prevent inflated correlations (Power et al., 2012). We used a threshold of 0.3 mm of average head displacement across all frames, including censored ones, during any scan to exclude subjects (one subject).

We reprocessed and reanalyzed data from Wang et al. (2014), which were acquired on a Siemens 3T TIM Trio with a 32-channel head coil. Structural (MPRAGE T1-weighted scans, TR = 2400 ms, TE = 3.16 ms, voxel size = 1 mm³, FOV = 25.6 cm, flip angle = 8°, 176 sagittal slices) and functional whole-brain BOLD EPI (TR = 2500 ms, TE = 20 ms, voxel size = 1.72 x 1.72 x 3 mm³, FOV = 22 cm, flip angle = 80°, 244 volumes, 10.2 minutes). We handled them identically to our own data, but resampled to 1.5 mm isotropic voxel resolution.

rTMS targeting

We based our targeting procedure on Wang et al. (2014) who chose the PPC subregion that was maximally connected to the hippocampus in each subject. They searched the anterior/middle hippocampus for the voxel with maximal FC to the PPC and chose the PPC location where this FC was strongest as the stimulation target. We applied a similar technique. For subjects receiving PPC stimulation, we guided rTMS to the PPC location with maximum FC to a seed location in the hippocampus. In each subject, the PPC target search volume was a sphere of 15 mm radius, cut to exclude non-brain voxels, around Talairach location x = -47, y = -68, z = +36, which included the supramarginal and angular gyri. The search for the hippocampal seed voxel involved two approaches, both employing automated scripts. For the first approach (12 subjects), we chose the maximally connected hippocampal voxel from six pre-selected

139 locations along the longitudinal aspect of the hippocampus in Talairach-Tournoux space (Seed
 140 1: $x = -26$, $y = -10$, $z = -17$; Seed 2: $x = -22$, $y = -16$, $z = -13$; Seed 3: $x = -30$, $y = -17$, $z = -14$;
 141 Seed 4: $x = -30$, $y = -22$, $z = -12$; Seed 5: $x = -30$, $y = -27$, $z = -9$; Seed 6: $x = -30$, $y = -32$, $z = -6$).
 142 This deviated from the seeding procedure of Wang et al. (2014), who sampled only from the
 143 anterior/middle hippocampus. In the second approach (3 subjects), we selected the maximally
 144 connected one of 97 pre-selected voxels in the anterior hippocampus. These included
 145 hippocampal voxels within 15 mm of the Talairach coordinates identified in Wang et al. (2014; x
 146 $= -24$, $y = -18$, $z = -18$). This approach was intended to provide wider sampling within the
 147 hippocampus. Figure 1 illustrates the seed locations for each subject. In both approaches, we
 148 created a 3 mm radius sphere around the coordinates of each voxel in the search and
 149 computed an average time series using the voxels in that sphere. We then searched the PPC
 150 sphere for the voxel with maximum correlation with the hippocampal seed, marked its location in
 151 standard space, and then back-transformed the location into subject space using the inverse
 152 matrix of the original affine transformation. Next, this location was transformed into a 3 mm
 153 radius sphere and overlaid on the subject's structural MRI for rTMS targeting with the Brainsight
 154 frameless stereotaxic system. For the PPC target, a stimulation trajectory was created in
 155 Brainsight, so that the plane of the coil was tangential to the scalp and the induced current field
 156 was oriented perpendicular to the long axis of the gyrus containing the stimulation target. For
 157 control stimulation, we located the vertex using the 10-20 International system (Steinmetz et al.,
 158 1989), and held the coil tangential to the scalp with the junction of the coil lobes in the sagittal
 159 axis.
 160
 161 *rTMS*
 162 TMS was delivered with a MagStim Rapid² stimulator through a Double Airfilm coil. (Wang et al.
 163 used a Nexstim eXimia NBS 4.3 air-cooled, MRI-guided system and a 70 mm figure eight coil.)
 164 rTMS intensity was referenced to the individual motor evoked potential threshold, which was

165 determined in the current experiment immediately before the first rTMS session using the TMS
166 Motor Threshold Assessment Tool (MTAT 2.0; <http://www.clinicalresearcher.org/software.htm>).
167 Stimulation parameter settings for PPC and vertex stimulation were identical to those of Wang
168 et al. (2014), i.e., 2-second trains at 20-Hz (40 pulses per train) with an inter-train interval of 28
169 sec, at 100% of resting motor threshold. There were 40 trains, 1600 pulses, and a duration of 20
170 min per session.

171

172 *FC calculations and voxel-wise analysis*

173 For all hippocampal FC analyses, we conducted the following steps: Preprocessed data from
174 the pre- and post- stimulation resting state scans were seeded at the hippocampal location
175 maximally connected with the PPC in the pre-stimulation scan, the area found for rTMS
176 targeting. We created a 3 mm radius sphere around this location and averaged the BOLD time
177 series of all voxels within it to derive a single hippocampal time series. Pearson's r-values were
178 then computed for the correlation between this time series and that from every voxel in the rest
179 of the brain. Finally, all r-values were r-to-z Fisher transformed to form a final connectivity metric
180 ($z_{(r)}$) across voxels for each scan.

181

182 Whole brain changes in hippocampal network FC and comparison to Wang et al. (2014)

183 To identify areas where PPC rTMS caused significant changes in hippocampal FC, and to see if
184 they were in the same areas reported by Wang et al. (2014), $z_{(r)}$ values for each subject and
185 time point, pre- and post-stimulation, were fed into AFNI's *3dttest++* command for comparison.
186 A group mask excluded ventricles and white matter. The results were false discovery rate (FDR)
187 corrected at $q = 0.05$. We applied Bonferroni corrected post-hoc tests to significant clusters in
188 regions where Wang et al. (2014) reported significantly greater hippocampal FC increases with
189 active compared to sham rTMS. These included the precuneus/retrosplenial, fusiform, lateral

190 parietal, and superior parietal areas ($\alpha = 0.05/4 = 0.0125$). Wilcoxon rank sum testing was used for
 191 significance testing since these data were non-normally distributed.

192

193 Hypothesis-based comparison to the Wang et al. (2014) results

194 We performed this analysis to see whether PPC rTMS in the current study caused significant
 195 increases in hippocampal FC within a mask of regions showing significant hippocampal FC
 196 change in the reanalyzed data of Wang et al. (2014). To determine this region-of-interest, we
 197 searched for areas of the posterior left hemisphere that showed a significant increase in
 198 hippocampal FC after active rTMS, relative to sham and calculated $z_{(r)}$ values as described
 199 above. For each subject in the data set of Wang et al. (2014), the pre-stimulation correlation
 200 map was subtracted from post-stimulation map, and the pre-sham map from the post-sham
 201 map. We then fed these subtractions into AFNI's *3dttest++* command for contrast. Like Wang et
 202 al. (2014), we applied a cluster size threshold of 290 voxels and identified a cluster
 203 encompassing the left precuneus and medial occipital lobe (left precuneus/occipital cortex;
 204 LPOC). We created a mask from these regions by applying the *3dclust* command in AFNI and
 205 resampling the mask to the geometry of our own data set (2 mm isotropic voxels). To account
 206 for variability across subjects, we dilated the mask by three voxels while restricting voxels to the
 207 left hemisphere. The pattern of results did not change based on the dilation of the mask. Finally,
 208 using the present data, we calculated pre- and post-stimulation hippocampal FC in these
 209 regions and contrasted the resulting pre- and post-stimulation $z_{(r)}$ values using a Wilcoxon rank
 210 sum test to look for a significant, PPC rTMS-related change in FC between the hippocampus
 211 and the LPOC region, like that reported by Wang et al. (2014).

212 We also calculated the change in hippocampus-LPOC FC with vertex rTMS. Here, we
 213 used the hippocampal seed that was maximally connected with the PPC target at baseline and
 214 the same automated script applied to the PPC subjects to avoid potential bias in the selection of

215 seeds. To determine whether changes in hippocampal FC with the LPOC mask were specific to
216 PPC stimulation, we compared the rTMS-related change in hippocampus-LPOC FC between
217 groups with a Mann-Whitney test. Additionally, to determine whether our results were affected
218 by differences in sample size between groups, we performed a permutation test using matched
219 sample sizes. This was performed by subtracting the mean FC change of the vertex group from
220 the mean FC change in eight subjects randomly selected from the PPC group. This was
221 performed 1,000 times to form a distribution of possible outcomes, which we then compared to
222 the observed mean difference.

223

224 Specificity analysis

225 To gauge the specificity of the Wang et al. (2014) effect on FC, we compared the changes in
226 hippocampal FC and global connectedness (GC) occurring in the LPOC mask (LPOC-GC) with
227 PPC rTMS. To calculate LPOC-GC, we found Pearson's r-values for each voxel in the brain for
228 the correlation of its time series with those of every other voxel. Next, we calculated the mean of
229 all of the r-values for each voxel within the LPOC mask (Gotts et al., 2012). The mean r-values
230 were then r-to-z Fisher transformed to create a GC value for each voxel. Finally, all voxel GC
231 values in the LPOC mask were averaged.

232 As an additional control, we calculated the change in FC between the left dorsolateral
233 prefrontal cortex (DLPFC) and the LPOC mask with the expectation that PPC stimulation would
234 not significantly enhance FC between these regions. We created the DLPFC seed by forming a
235 3 mm radius sphere around Talairach and Tournoux location $x = -41$, $y = 44$, $z = 5$, a peak area
236 of activation found during procedural learning (Poldrack et al., 2001). The mean time series from
237 this sphere was then compared with that from every voxel in the LPOC mask. Finally, we took
238 the mean of all r-to-z transformed values in the LPOC mask. Wilcoxon rank sum tests were

performed to determine if the hippocampal-LPOC FC change differed significantly from the DLPFC-LPOC FC and LPOC-GC changes.

Comparison of topographic changes

We assessed the topographic pattern of hippocampal FC changes from PPC stimulation by calculating the change in hippocampal FC with 17 segregated networks (Yeo et al., 2011) using AFNI's *3dBrickStat* command. We also calculated within-network GC for this analysis using the time series of all voxels in each of the 17 networks. GC for each network was calculated as the mean $z_{(t)}$ value across all voxels in that network. We then compared the hippocampal FC and GC changes. The same steps were performed using the pre- to post- active stimulation data from Wang et al. (2014). We performed hippocampal-FC to GC comparisons for each study with one-sample, two-tailed t-tests, since these data were normally distributed.

Finally, to test the hypothesis that the magnitude of hippocampal FC changes across networks were correlated across studies, we conducted a simple correlation analysis to test this hypothesis ($\alpha = 0.05$).

Correlation between baseline hippocampal FC and rTMS-induced changes in FC amongst hippocampal network nodes.

The purpose of this analysis was to determine whether we could reproduce the finding of Wang et al. (2014) that baseline hippocampal FC predicted the degree of PPC rTMS-induced change in hippocampal FC among brain areas. We first found clusters of voxels in our data where rTMS produced a significant increase in hippocampal FC at a threshold of $p < 0.01$, with no spatial extent threshold. Like Wang et al. (2014), we applied a liberal threshold in order to include a range of change values. This resulted in 183 significant clusters, which we then divided into Automated Anatomical Labeling (AAL; Tzourio-Mazoyer et al., 2002)-defined anatomical regions

264 and all regions with greater than 15 voxels were included in the analysis. The 15-voxel threshold
265 was applied to ensure that each cluster contained enough voxels to calculate a reliable mean
266 time series. This resulted in 95 clusters. We then formed a correlation matrix for each subject
267 and time point by comparing the mean time series of each cluster with that of each other cluster
268 (*3dNetCorr*). Next, we averaged the correlation matrices within each time point across subjects
269 and subtracted the pre-stimulation correlation matrix from the post-stimulation matrix. This
270 resulted in a single matrix, which we sorted by baseline hippocampal FC. Then, to determine if
271 baseline hippocampal FC predicted the rTMS-induced change in FC, we plotted the baseline
272 hippocampal FC of each cluster against the mean change in FC between that cluster and every
273 other cluster. Finally, to determine whether these changes were specific to FC with the
274 hippocampus, we performed the same analyses, but replaced hippocampal FC with GC for
275 each cluster. Additionally, we re-sorted these matrices by region to reveal, qualitatively, areas
276 where hippocampal nodes and nodes that increased in GC, showed the highest change in FC.

277

278 *Statistical Analyses*

279 All analyses were conducted using R software. Shapiro-Wilks tests of normality were conducted
280 prior to each analysis. Table 1 lists the specifications of each test, including critical values, the
281 data used in each test, and confidence intervals. In the Results, an alphabetic code is listed with
282 each test linking it to additional details in Table 1.

283

Results

The interval between rTMS sessions was 23.9 ± 3.0 hours for the PPC group and 24.3 ± 2.7 hours for the vertex group (non-significant; Table 1, a, $W = 36$, $p = 0.327$, 95% CI [-0.0743 0.2110]). Head motion, calculated as average head frame displacement in six directions, did not significantly differ between scans (pre- vs. post-stimulation; Table 1, b, $V = 167$, $p = 0.194$, 95% CI [-0.0743 0.2110]) or groups (Parietal vs. Vertex; Table 1, c, $W = 199.5$, $p = 0.350$, 95% CI [-0.0225 0.0096]). The same was true for the number of censored TRs during denoising (pre- vs. post-stimulation; Table 1, d, $V = 118.5$, $p = 0.155$, 95% CI [-0.9999 6.5000]; Parietal vs. Vertex; Table 1, e, $W = 218.5$, $p = 0.604$, 95% CI [-3.0000 0.00004]). Average head displacement was 0.089 ± 0.005 mm per frame. The average number of censored TRs per scan was 5.348 ± 1.561 .

Figure 2 shows regions that changed in FC with the hippocampus (FDR corrected, $q = 0.05$) in the current sample. These changes were all increases. PPC rTMS produced significant increases in hippocampal FC in all of the areas reported by Wang et al. (2014), including left retrosplenial cortex (Table 1, f, $V = 7$, $p = 1.16 \times 10^{-3}$, 95% CI [0.0654, 0.2590]), left fusiform gyrus (Table 1, g, $V = 4$, $p = 4.27 \times 10^{-4}$, 95% CI [0.0951 0.2132]), left lateral parietal cortex (Table 1, h, $V = 1$, $p = 1.22 \times 10^{-4}$, 95% CI [0.0777 0.2034]), left superior parietal cortex (Table 1, i, $V = 2$, $p = 1.83 \times 10^{-4}$, 95% CI [0.0815 0.2294]; all results Bonferroni corrected).

In our reanalysis of the Wang et al. data (2014), the LPOC region of interest showed significantly increased FC with the hippocampus after active rTMS, relative to sham. In the current sample, we also found that PPC rTMS caused significant increases there (Table 1, j, $V = 95$, $p = 0.048$, 95% CI [0.0013 0.2053]; Fig. 3A). This increase ($z_{(r)} = 0.20 \pm 0.04$; $\text{mean}_{(\text{SEM})}$) was larger than, and opposite in direction to, the mean change after vertex rTMS ($z_{(r)} = -0.08 \pm 0.06$; Fig 3A). The changes in the PPC rTMS group were significantly greater than the changes in the vertex group (Table 1, k, $W = 93$, $p = 0.034$, 95% CI [0.0195 0.3257]). Vertex stimulation did not cause changes in hippocampal-LPOC FC (Table 1, l, $V = 7$, $p = 0.148$, 95% CI [-0.055. 0.2357]). Resampling the group differences in hippocampal-LPOC FC in 1,000

310 matched groups of eight subjects showed no instances where changes were greater in the
 311 vertex group, including those bounded by 95% of the distribution (Table 1, m, observed mean =
 312 0.1795, 95% of distribution [0.02513 0.03392]; see Fig. 4). Thus, it is unlikely that our results
 313 were driven by differences in sample size between groups. Whole-brain analyses of
 314 hippocampal FC changes in the vertex group did not reveal any significant clusters (all $p >$
 315 0.05). The same was true when measuring FC from the vertex stimulation site.

316 In the current data, DLPFC-LPOC FC did not increase significantly after PPC rTMS
 317 (Table 1, n, $V = 81$, $p = 0.2524$, 95% CI [-0.0344 0.1270]; Fig. 3A), but the DLPFC-LPOC FC
 318 change did not differ significantly from the hippocampal-LPOC FC change (Table 1, o, $V = 75$, p
 319 $= 0.4212$, 95% CI [-0.0636 0.1593]), nor did LPOC-GC (Table 1, p, $V = 94$, $p = 0.055$, 95% CI [-
 320 0.0006 0.04139]). However, there was a trend-level difference between the GC and
 321 hippocampal FC changes in the LPOC region (Table 1, q, $V = 92$, $p = 0.073$, 95% CI [-0.0066
 322 0.1547]). We conducted additional control analyses to determine whether stimulation caused
 323 significant increases in FC between the DFLPC and the hippocampus, but it did not (Table 1, r,
 324 $t(14) = 0.949$, $p = 0.359$, 95% CI [-0.061 0.157]), nor were there changes in FC between the
 325 DLPFC and the stimulus location in the PPC (Table 1, s, $V = 68$, $p = 0.679$, 95% CI [-0.103
 326 0.121]), nor did PPC-GC increase (Table 1, t, $V = 92$, $p = 0.073$, 95% CI [-0.005 0.050]).

327 In the current sample, there was an increase in hippocampal FC with the 17 networks
 328 identified by Yeo et al. (2011), which was significantly stronger than the GC changes in these
 329 networks (Table 1, u, $T_{(16)} = 10.96$, 7.6×10^{-9} , 95% CI [0.0725 0.1073]). We found the same
 330 effect in the data from Wang et al. (Table 1, v, $T_{(16)} = 11.27$, $p = 5.10 \times 10^{-9}$, 95% CI [0.0138
 331 0.0201]; Fig. 3B). Comparing the hippocampal FC changes between studies, we found that they
 332 were larger in the current study, despite using fewer stimulation sessions (Table 1, w, $T_{(32)} =$
 333 8.75 , $p = 5.42 \times 10^{-10}$, 95% CI [0.0560 0.09]), although GC changes were also larger in the
 334 current results than in the Wang et al. data, suggesting overall differences in the magnitude of
 335 FC changes across experiments, which could reflect factors such as different scan variables

336 between studies. After PPC stimulation in both studies, increases in hippocampal FC were
337 maximal in networks that included the cuneus and retrosplenial, somatosensory, and superior
338 temporal areas (Fig. 5).

339 In our test for whether the whole-brain topographic patterns of rTMS-induced
340 hippocampal FC were similar between studies, we found that FC changes were correlated
341 between studies (Table 1, x, $r = 0.51$, $n = 17$, $p = 0.037$, 95% CI [0.0389 0.7956]; Fig. 6). There
342 was no significant correlation between the GC changes in the current study with the
343 hippocampal FC changes of Wang et al. (Table 1, y, $r = 0.16$, $n = 17$, $p = 0.536$, 95% CI [-0.3419
344 0.5989]). These results indicate that the magnitude of hippocampal FC changes across
345 networks was similar between studies, and that their topographic distribution was reproducible.

346 Finally, we reproduced the finding that, among areas showing significant increases in
347 hippocampal FC after PPC rTMS, pre-stimulation hippocampal FC predicted the magnitude of
348 the increase (Fig 7A). This was confirmed by the relationship between the baseline and mean
349 change in hippocampal FC across areas (Table 1, z, $r = 0.39$, $n = 95$, $p = 1.0 \times 10^{-4}$, 95% CI
350 [0.2002 0.5453]; Fig. 8A). Removing the single outlier did not change the significance of the
351 correlation (Table 1, aa, $r_{(92)} = 0.47$, $p = 1.14 \times 10^{-6}$, 95% CI [0.2955 0.6141]). We did not
352 observe the same pattern of results when performing the same analyses using GC as the
353 dependent variable (Table 1, bb, $r = -0.08$, $n = 115$, $p = 0.39$, 95% CI [-0.2593 0.1046]; Figs. 7B
354 and 8B). These findings indicate a specific effect of PPC rTMS on the hippocampus and rule out
355 non-specific enhancement of FC across the brain. Re-sorting the matrices in Fig. 7 revealed no
356 regional differences in the change in GC (Fig. 7B), but did show that, among regions connected
357 to the hippocampus at baseline, frontal regions showed qualitatively less change than more
358 posterior regions, such as the parietal cortex, similar to the results of Wang et al. (2014) and
359 consistent with the interpretation that areas with higher baseline FC with the hippocampus
360 change most with PPC rTMS.

Discussion

We independently reproduced the highly specific increase in hippocampal FC, reported by Wang et al. (2014), resulting from high-frequency rTMS of PPC, using a partial replication of their technique and adding additional new controls. We applied a whole-brain analysis as well as a hypothesis-based approach, predicated on the anatomical distribution of changes reported by Wang et al. (2014). We also looked for changes in hippocampal FC within 17 additional segregated brain networks (Yeo et al., 2011). The whole-brain comparison to Wang et al. (2014) revealed that PPC rTMS caused significant hippocampal FC changes in all of the regions reported by Wang et al, as well as several others. The hypothesis-based approach revealed significant increases in hippocampal FC with the LPOC, a region derived from our re-analysis of the Wang et al. (2014) data. These changes were specific to FC with the hippocampus: PPC rTMS did not significantly increase FC between the DLPFC, an area active in many cognitive processes, including learning, and the LPOC. We also ruled out the possibility that the findings reflected a general increase in brain connectivity: Hippocampal FC was significantly greater than GC across all networks examined in both the present and the Wang et al. data. Although our vertex control sample was small, we found no significant FC changes in this group, and hippocampus-LPOC FC was significantly greater for the PPC rTMS group than the vertex group.

As in the data of Wang et al. (2014), baseline hippocampal FC predicted PPC rTMS-induced FC changes and we demonstrated the specificity of this relationship by showing that baseline GC did not predict GC increases after rTMS. Finally, the spatial pattern of rTMS-induced FC change was similar and correlated between studies. Taken together this is strong evidence that the effect of 20 Hz rTMS on the PPC on hippocampal FC is robust, reproducible, and highly specific in anatomical terms.

Notably, we were able to reproduce and possibly to exceed the results of Wang et al. (2014) with fewer stimulation sessions. Multiple consecutive rTMS sessions are burdensome to

387 subjects and investigators alike and reducing the requirement increases the attractiveness of
388 the PPC rTMS paradigm.

389 Our vertex rTMS group showed decreased hippocampal FC with almost every network,
390 including the LPOC. This unexplained time-related drift could be due to a physiological effect
391 and might represent a potential confound. However, as noted above, others (Jung et al., 2016)
392 have found no evidence of FC changes from vertex rTMS. Additionally, the average change in
393 hippocampal FC across the networks from Yeo et al. (2011) in the Wang et al. (2014) sham
394 data did not differ significantly from zero.

395 There were several procedural differences between the current work and that of Wang
396 et al. (2014), the most obvious of which was the absence of behavioral testing. Therefore, we do
397 not know whether the changes in hippocampal FC were associated with an improvement in
398 declarative memory. Additionally, there were differences in how we preprocessed our resting-
399 state data. We did not bandpass filter our data. Unlike Wang et al. (2014), we included spatial
400 smoothing to reduce the influence of spatial noise and increase signal-to-noise ratio (SNR).

401 Another difference between studies was our use of a vertex stimulation control. Wang et
402 al. (2014), used subthreshold stimulation (10% of resting motor threshold; RMT) to the PPC as
403 their within-subjects control, which may have caused weak local brain effects without
404 reproducing the somatosensory effect of full-intensity rTMS. They also used full-intensity
405 stimulation of the motor cortex in an independent group as a secondary control and this was all
406 but certain to produce widespread changes in FC. We chose active-intensity stimulation at the
407 vertex as our control because others (Jung et al., 2016) found no effect on FC from stimulation
408 there and it lies over the sagittal sinus and the interhemispheric fissure, where the cortex is
409 relatively distant from the coil and the nearest regions out of the plane of the stimulating current.
410 Neither in this, nor the study of Wang et al. (2014), did control stimulation produce any
411 measurable increase in hippocampal FC.

412 Finally, for reasons described above, we used three and, in some cases, four days of
413 rTMS, while Wang et al. (2014) used five. This study contains no basis for a quantitative
414 comparison of the strength or duration of the connectivity or behavioral changes produced by
415 various treatment durations, but 3-4 days appeared adequate to produce FC changes similar to
416 those of Wang et al. (2014) at a 24 hour delay. These procedural differences do not allow us to
417 claim a strict replication of the paradigm, but they do not detract from the substantial
418 reproduction of the result and could not have caused it by themselves.

419 Both we and Wang et al. (2014) were able to produce dramatic increases in
420 hippocampal network FC with a few sessions of PPC rTMS, making this one of the strongest
421 and most reliable effects in noninvasive neuromodulation. The differences in the treatment
422 paradigms and image processing procedures decrease the likelihood that both studies arrived
423 at a similar result due to an artifact or systematic noise. Others (Gratton et al., 2013; Rahnev et
424 al., 2013; Rastogi et al., 2017; Steel et al., 2016; van der Werf et al., 2010; Vercammen et al.,
425 2010) have also used FC to study how rTMS affects brain function at the network level. FC in
426 the default mode network appears to be particularly sensitive to modulation with rTMS (Eldaief
427 et al., 2011; Halko et al., 2014; Wang et al., 2014) and can be modulated by stimulating the
428 PPC (Eldaief et al., 2011; Wang et al., 2014) and the cerebellum (Halko et al., 2014). The latter
429 study also used individual FC to choose the the stimulation target.

430 Future studies may consider examining whether the stimulation regimen itself, largely
431 inspired by conventional rTMS treatment for depression (e.g., George et al., 1997), where it was
432 adopted without systematic exploration of the parameter space, is optimal, and whether even
433 more dramatic or faster responses are attainable using optimized stimulation parameter
434 settings.

435

Conclusion

436
437 The hippocampal network FC changes reported by Wang et al. (2014) after PPC rTMS, are
438 reproducible in magnitude, specificity, and topographic distribution. Our additional analyses,
439 ruling out changes in global correlation, further strengthen the evidence for the selectivity
440 approach for the hippocampal network. Moreover, our findings suggest that these effects are
441 achievable with fewer than five stimulation sessions. This provides encouraging support for PPC
442 rTMS as a means of enhancing memory network FC and for rTMS in general as a technique for
443 producing targeted changes in brain network connectivity.

References

- Baraduc P, Lang N, Rothwell JC, Wolpert DM (2004) Consolidation of dynamic motor learning is not disrupted by rTMS of primary motor cortex. *Curr Biol* 14:252–256.
- Cavada C, Goldman-Rakic PS (1989) Posterior parietal cortex in rhesus monkey: I. Parcellation of areas based on distinctive limbic and sensory corticocortical connections. *J Comp Neurol* 287:393–421.
- Cox RW (1996) AFNI : Software for analysis and visualization of functional magnetic resonance neuroimages. *Comput Biomed Res* 29:162–173.
- Eldaief MC, Halko MA, Buckner RL, Pascual-leone A (2011) Transcranial magnetic stimulation modulates the brain's intrinsic activity in a frequency-dependent manner. *Proc from Natl Acad Sci* 108:21229–21234.
- George MS, Wassermann EM, Kimbrell TA, Little JT, Williams WE, Danielson AL, Greenberg BD, Hallett M, Post RM (1997) Mood improvement following daily left prefrontal repetitive transcranial magnetic stimulation in patients with depression: A placebo-controlled crossover trial. *Am J Psychiatry* 154:1752–1756.
- Gotts SJ, Simmons WK, Milbury LA, Wallace GL, Cox RW, Martin A (2012) Fractionation of social brain circuits in autism spectrum disorders. *Brain* 135:2711–2725.
- Gratton C, Lee TG, Nomura EM, Esposito MD, Halko MA, Israel B (2013) The effect of theta-burst TMS on cognitive control networks measured with resting state fMRI. *Front Syst Neurosci* 7:1–14.
- Halko MA, Farzan F, Eldaief MC, Schmahmann JD, Pascual-Leone A (2014) Intermittent theta-burst stimulation of the lateral cerebellum increases functional connectivity of the default network. *J Neurosci* 34:12049–12056.
- Héroux ME, Taylor JL, Gandevia SC (2015) The use and abuse of transcranial magnetic stimulation to modulate corticospinal excitability in humans. *PLoS One* 10:1–10.
- Hotermans C, Peigneux P, De Noordhout AM, Moonen G, Maquet P (2008) Repetitive

transcranial magnetic stimulation over the primary motor cortex disrupts early boost but not
 delayed gains in performance in motor sequence learning. *Eur J Neurosci* 28:1216–1221.

Iezzi E, Suppa A, Conte A, Agostino R, Nardella A, Berardelli A (2010) Theta-burst stimulation
 over primary motor cortex degrades early motor learning. *Eur J Neurosci* 31:585–592.

Jung J, Bungert A, Bowtell R, Jackson SR (2016) Vertex stimulation as a control site for
 transcranial magnetic stimulation : A concurrent TMS/fMRI study. *Brain Stimul* 9:58–64.

Mesulam MM, Van Hoesen GW, Pandya DN, Geschwind N (1977) Limbic and sensory
 connections of the inferior parietal lobule (area PG) in the rhesus monkey: A study with a
 new method for horseradish peroxidase histochemistry. *Brain Res* 136:393–414.

Muellbacher W, Ziemann U, Wissel J, Dang N, Kofler M, Facchini S, Boroojerdi B, Poewe W,
 Hallett M (2002) Early consolidation in human primary motor cortex. *Nature* 415:640–644.

Nahas ZH, George MS, Schlaepfer TE, Marcolin MA, O'Reardon JP, Padberg F, Fitzgerald PB
 (2008) Controversy: Repetitive transcranial magnetic stimulation or transcranial direct
 current stimulation shows efficacy in treating psychiatric diseases (depression, mania,
 schizophrenia, obsessive-compulsive disorder, panic, posttraumatic stress disorder). *Brain*
Stimul 2:14–21.

Nestor PJ, Fryer T, Hodges JR (2005) Declarative memory impairments in Alzheimer's disease
 and semantic dementia semantic dementia. *Neuroimage* 30:1010–1020.

Poldrack RA, Clark J, Pare-Blagoev EJ, Shohamy D, Moyano JC, Myers C, Gluck MA (2001)
 Interactive memory systems in the human brain. *Nature* 414:546–550.

Poldrack RA, Matthews PM, Gorgolewski KJ, Baker CI, Munafò MR, Vul E, Yarkoni T, Nichols
 TE, Durnez J, Poline J-B (2017) Scanning the horizon: Towards transparent and
 reproducible neuroimaging research. *Nat Rev Neurosci* 18:115–126.

Power JD, Barnes KA, Snyder AZ, Schlaggar BL, Petersen SE (2012) Spurious but systematic
 correlations in functional connectivity MRI networks arise from subject motion. *Neuroimage*
 59:2142–2154.

- 496 Rahnev D, Kok P, Munneke M, Bahdo L, Lange FP De, Lau H (2013) Continuous theta burst
497 transcranial magnetic stimulation reduces resting state connectivity between visual areas. *J*
498 *Neurophysiol* 110:1811–1821.
- 499 Rastogi A, Cash R, Dunlop K, Vesia M, Kucyi A, Ghahremani A, Downar J, Chen J, Chen R
500 (2017) Modulation of cognitive cerebello-cerebral functional connectivity by lateral
501 cerebellar continuous theta burst stimulation. *Neuroimage* 158:48–57.
- 502 Rosenthal CR, Roche-kelly EE, Husain M, Kennard C (2009) Response-dependent
503 contributions of human primary motor cortex and angular gyrus to manual and perceptual
504 sequence learning. *J Neurosci* 29:15115–15125.
- 505 Rossi S et al. (2009) Safety, ethical considerations, and application guidelines for the use of
506 transcranial magnetic stimulation in clinical practice and research. *Clin Neurophysiol*
507 120:2008–2039.
- 508 Shirer WR, Jiang H, Price CM, Ng B, Greicius MD (2015) Optimization of rs-fMRI pre-
509 processing for enhanced signal-noise separation, test-retest reliability, and group
510 discrimination. *Neuroimage* 117:67–79.
- 511 Steel A, Song S, Bageac D, Knutson KM, Keisler A, Saad ZS, Gotts SJ, Wassermann EM,
512 Wilkinson L (2016) Shifts in connectivity during procedural learning after motor cortex
513 stimulation: A combined transcranial magnetic stimulation/functional magnetic resonance
514 imaging study. *Cortex* 74:134–148.
- 515 Steinmetz H, Fürst G, Meyer BU (1989) Craniocerebral topography within the international 10-
516 20 system. *Electroencephalogr Clin Neurophysiol* 72:499–506.
- 517 Talairach P, Tournoux J (1988) A stereotactic coplanar atlas of the human brain. New York:
518 Thieme.
- 519 Teo JTH, Swayne OBC, Cheeran B, Greenwood RJ, Rothwell JC (2011) Human theta burst
520 stimulation enhances subsequent motor learning and increases performance variability.
521 *Cereb Cortex* 21:1627–1638.

- 522 Thut G, Pascual-leone A (2010) A review of combined TMS-EEG studies to characterize lasting
 523 effects of repetitive TMS and assess their usefulness in cognitive and clinical
 524 neuroscience. *Brian Topogr* 22:219–232.
- 525 Tzourio-Mazoyer N, Landeau B, Papathanassiou D, Crivello F, Etard O, Delcroix N, Mazoyer B,
 526 Joliot M (2002) Automated anatomical labeling of activations in SPM using a macroscopic
 527 anatomical parcellation of the MNI MRI single-subject brain. *Neuroimage* 15:273–289.
- 528 Vakil E (2005) The effect of moderate to severe traumatic brain injury (TBI) on different aspects
 529 of memory: A selective review. *J Clin Exp Neuropsychol* 27:977–1021.
- 530 van der Werf Y, Sanz-arigita EJ, Menning S, van den Heuvel OA (2010) Modulating
 531 spontaneous brain activity using repetitive transcranial magnetic stimulation. *BMC*
 532 *Neurosci* 11:145.
- 533 Vercammen A, Knegtering H, Liemburg E, den Boer A, Aleman A (2010) Functional connectivity
 534 of temporo-parietal region in schizophrenia: Effects of rTMS treatment of auditory
 535 hallucinations. *J Psychiatr Res* 44:725–731.
- 536 Wang JX, Rogers LM, Gross EZ, Ryals AJ, Dokucu ME, Brandstatt KL, Hermiller MS, Voss JL
 537 (2014) Targeted enhancement of cortical-hippocampal brain networks and associative
 538 memory. *Science* 345:1054–1057.
- 539 Wang JX, Voss JL (2015) Long-lasting enhancements of memory and hippocampal-cortical
 540 functional connectivity following multiple-day targeted noninvasive stimulation.
 541 *Hippocampus* 25:877–883.
- 542 Wilkinson L, Steel A, Mooshagian E, Zimmermann T, Keisler A, Lewis JD, Wassermann EM
 543 (2015) Online feedback enhances early consolidation of motor sequence learning and
 544 reverses recall deficit from transcranial stimulation of motor cortex. *Cortex* 71:134–147.
- 545 Wilkinson L, Teo JT, Obeso I, Rothwell JC, Jahanshahi M (2010) The contribution of primary
 546 motor cortex is essential for probabilistic implicit sequence learning: Evidence from theta
 547 burst magnetic stimulation. *J Cogn Neurosci* 22:427–436.

548 Yeo BT, Krienen FM, Sepulcre J, Sabuncu MR, Lashkari D, Hollinshead M, Roffman JL, Smoller
549 JW, Zollei L, Polimeni JR, Fischl B, Liu H, Buckner RL (2011) The organization of the
550 human cerebral cortex estimated by intrinsic functional connectivity. *J Neurophysiol*
551 106:1125–1165.
552

Table Caption

553
554 Table 1. Statistics table indicating the results of all analyses. Each analysis includes a letter
555 indicator ("Manuscript" column) linking the test in the table to the analysis in the text. The link to
556 the corresponding figure, if any, and the sample used for the test are indicated in the "Figure,"
557 and "Sample," columns respectively. The "Current" sample includes tests using data from the
558 current work, and the previous study is indicated as "Wang et al. (2014)." The dependent
559 variables for each test are listed as "Data Type," and the "Data Structure" column indicates
560 whether the data are normally distributed. The type of test, contrast, and the groups used for the
561 analysis are listed in the "Type of test" column. The multiple correction method is listed under
562 "Multiple comparisons correction." The program used to perform the analysis is included under
563 "Program." The critical value and degrees of freedom are listed for each test under "Statistics."
564 Finally, the p-value and confidence intervals are listed in the final two columns. DLPFC =
565 Dorsolateral Prefrontal Cortex; GC = Global Connectedness; LPOC = Left Precuneus and
566 Medial Occipital Cortex.

Figure Captions

567

568

569 Figure 1. Seed locations from PPC (Top; N=15) and vertex groups (Bottom; N=8).

570 Figure 2. Regions showing significant change in hippocampal FC following PPC rTMS from the

571 current study (FDR corrected, $q = 0.05$).

572 Figure 3. A. Average change in hippocampal-LPOC FC for subjects receiving PPC stimulation

573 (left bar) and vertex stimulation (middle bar). Average DLPFC-LPOC FC changes for subjects

574 receiving PPC stimulation is represented by the right bar. B. Mean changes in hippocampal FC

575 within 17 segregated networks from Yeo et al. (2011) after PPC rTMS in this study and Wang et

576 al. and change in GC within networks from both studies. Error bars represent the standard error

577 of the mean. * - $p < 0.05$, * - $p < 0.0001$.

578 Figure 4. Histogram representing the result of 1,000 group mean differences using 8 subjects

579 from each group, where the 8 PPC subjects are randomly sampled each time. The black dotted

580 lines represent the upper (0.2536) and lower (0.1098) limit of 95% of the distribution. The

581 observed mean difference between the PPC and vertex group is shown by the red line (0.1795).

582 Figure 5. Effect size of increases in hippocampal FC within three representative networks from

583 Yeo et al. (2011) after PPC rTMS in this study and Wang et al. Network 1 includes cuneus and

584 retrosplenial cortex. Network 2 includes somatosensory areas. Network 3 includes superior

585 temporal areas.

586 Figure 6. Scatterplot of PPC rTMS-induced hippocampal FC ($z_{(r)}$) changes across networks from

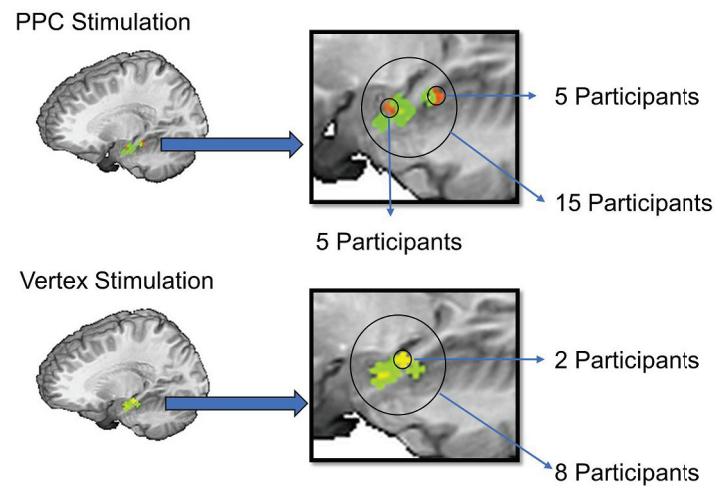
587 Yeo et al. (2011). Each dot represents the rTMS-induced hippocampal FC change from the

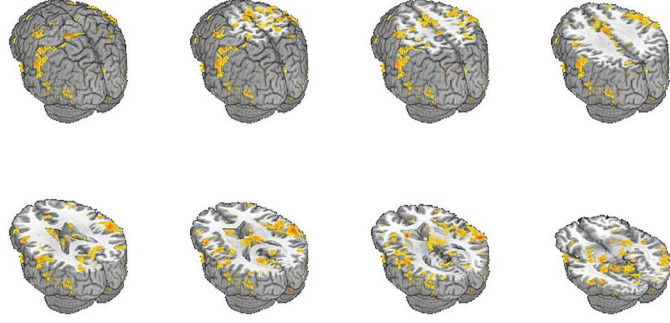
588 current study (x-axis) and Wang et al. (y axis) within one of the 17 networks from Yeo et al.

589 (2011). The black line represents the regression line across individual data points.

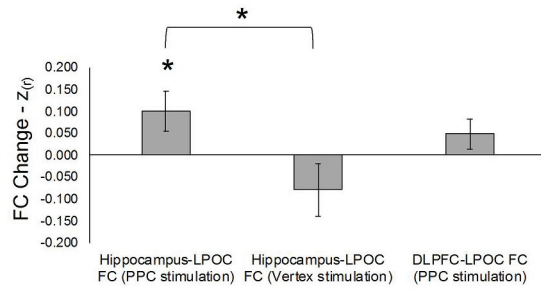
590 Figure 7. Correlation matrices of regions demonstrating significant ($p < 0.01$) changes in
591 hippocampal (A) and global (B) FC. Matrices are sorted by baseline FC with the highest values
592 represented at the top of the matrices on the y-axis and to the left on the x-axis. Color bars
593 aligned with each axis represent AAL-defined regions. Panels C and D are identical to Panels A
594 and B, but are sorted by region.

595 Figure 8. A. Scatterplot of baseline hippocampal FC for regions demonstrating significant ($p <$
596 0.01) changes in hippocampal FC and average rTMS-induced FC change in those regions. B.
597 Scatterplot of baseline GC for regions demonstrating significant ($p < 0.01$) changes in GC and
598 average rTMS-induced internode GC change in those regions.

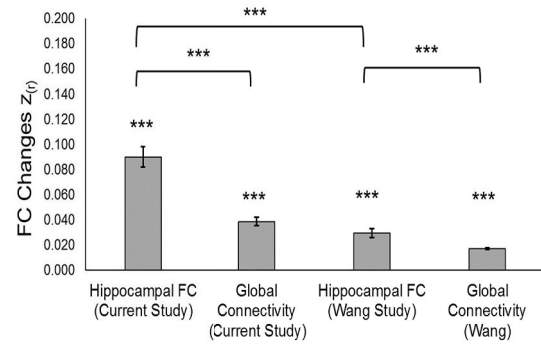


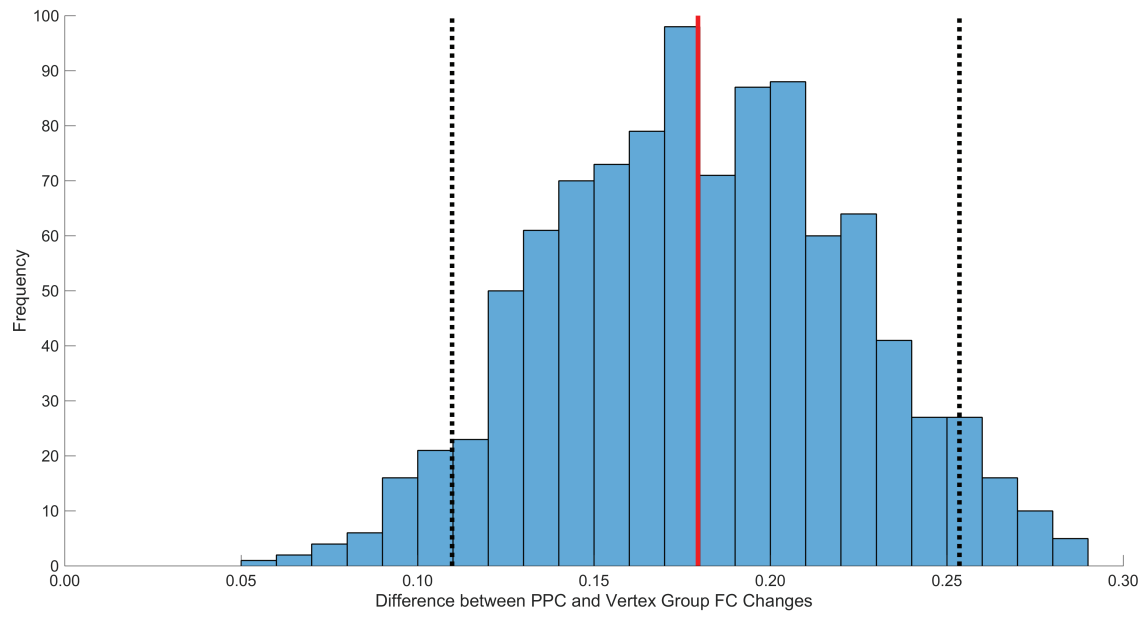


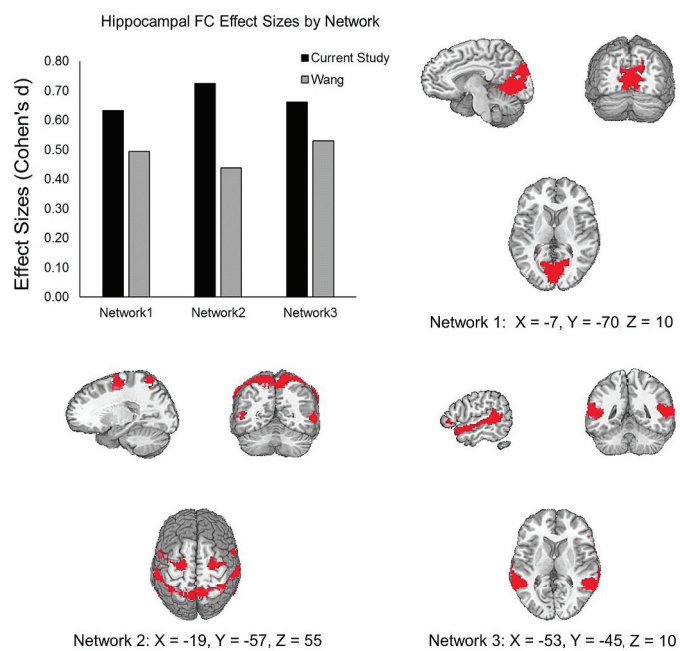
A)

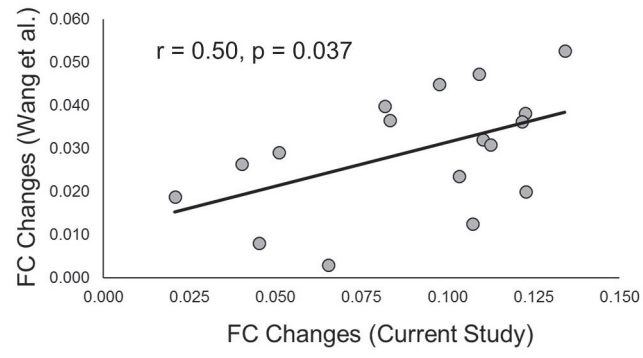


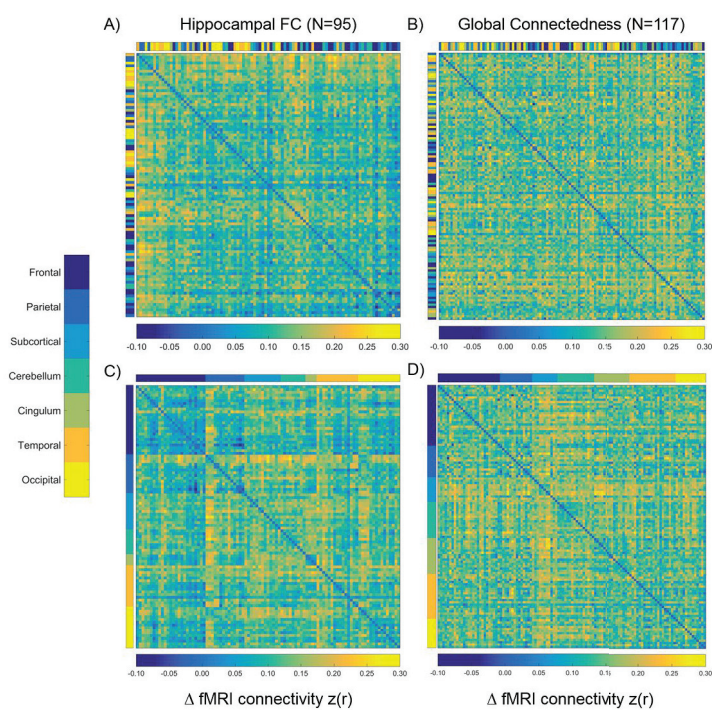
B)

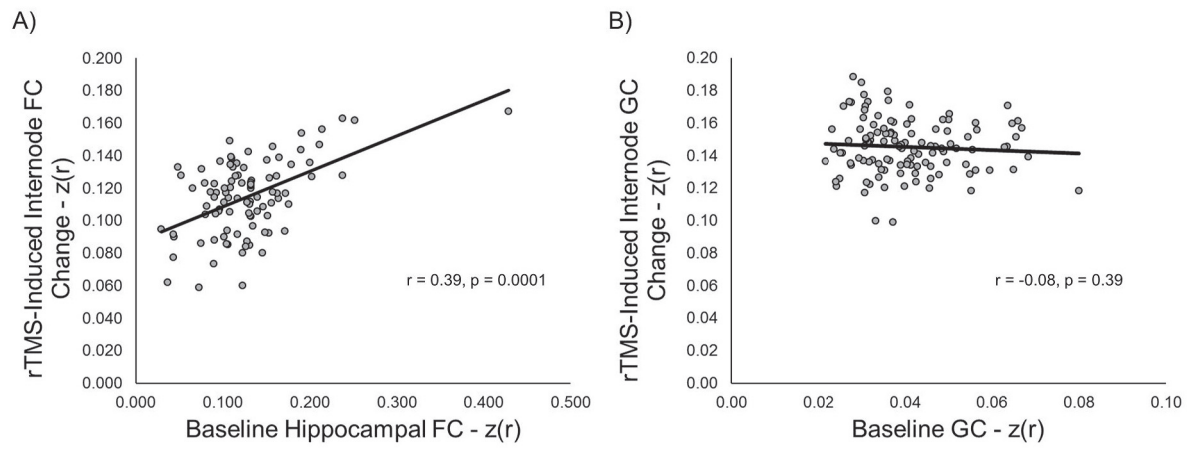












Manuscript	Figure	Sample	Data type	Data structure	Type of test	Multiple comparison correction	Program	Statistics	p values	Confidence Intervals
a		Current	Spacing between stimulation sessions	Non-normal distribution	Mann-Whitney (between groups; PPC group: Participants receiving 3 vs. 4 days of stimulation)		R	W = 36	p = 0.327	mean = 0.1092, 95% CI [-0.0743 0.2110]
b		Current	Average motion displacement	Non-normal distribution	Wilcoxon Rank Sum (all subjects; post vs. pre)		R	V = 167	p = 0.194	Mean = 0.0074 95% CI [-0.0032 0.0204]
c		Current	Average motion displacement	Non-normal distribution	Mann-Whitney (Parietal vs. Vertex)		R	W = 199.5	p = 0.350	Mean = -0.0099 95% CI [-0.0225 0.0096]
d		Current	Number of censored trials	Non-normal distribution	Wilcoxon Rank Sum (all subjects; post vs. pre)		R	V = 118.5	p = 0.155	Mean = 2.5000 95% CI [-0.9999 6.5000]
e		Current	Number of censored trials	Non-normal distribution	Mann-Whitney (Parietal vs. Vertex)		R	W = 218.5	p = 0.604	Mean = -2.1121 95% CI [-3.0000 0.00004]
f	2	Current	Whole-brain FC analysis - retrosplenial cortex	Non-normal distribution	Wilcoxon Rank Sum (within-groups; PPC group - post-hoc test, post vs. pre active stimulation)	Bonferroni	R	V = 7	p = 1.16 x 10 ⁻³	mean = 0.1697, 95% CI [0.0654 0.2590]
g	2	Current	Whole-brain FC analysis - fusiform gyrus	Non-normal distribution	Wilcoxon Rank Sum (within-groups; PPC group - post-hoc test, post vs. pre active stimulation)	Bonferroni	R	V = 4	p = 4.27 x 10 ⁻⁴	mean = 0.1475, 95% CI [0.0951 0.2132]
h	2	Current	Whole-brain FC analysis - lateral parietal cortex	Non-normal distribution	Wilcoxon Rank Sum (within-groups; PPC group - post-hoc test, post vs. pre active stimulation)	Bonferroni	R	V = 1	p = 1.22 x 10 ⁻⁴	mean = 0.1331, 95% CI [0.0777 0.2034]
i	2	Current	Whole-brain FC analysis - superior parietal cortex	Non-normal distribution	Wilcoxon Rank Sum (within-groups; PPC group - post-hoc test, post vs. pre active stimulation)	Bonferroni	R	V = 2	p = 1.83 x 10 ⁻⁴	mean = 0.1682, 95% CI [0.0815 0.2294]
j	3A	Current	Hippocampal-LPOC FC changes (a priori)	Non-normal distribution	Wilcoxon Rank Sum (within-groups; PPC group - post vs. pre active stimulation)		R	V = 95	p = 0.048	mean = 0.0867, 95% CI [0.0013 0.2053]
k	3A	Current	Hippocampal-LPOC FC	Non-normal	Mann-Whitney (between groups;)		R	W = 93	p = 0.034	mean = 0.1367, 95% CI [0.0195 0.3257]

			changes (a priori)	distribution	PPC group vs. Vertex group)					
l	4	Current	Hippocampal-LPOC FC changes	Non-normal distribution	Permutation Test (between groups; PPC group vs. Vertex group)	R	Observed mean difference = 0.1795			95% of distribution [0.1098 0.2536]
m	3A	Current	Hippocampal-LPOC FC changes (a priori)	Non-normal distribution	Wilcoxon Rank Sum (within groups; Vertex group - post vs. pre active stimulation)	R	V = 7	p = 0.148		mean = -0.0477, 95% CI [-0.0554 0.2357]
n	3A	Current	DLPFC-LPOC FC changes (a priori)	Non-normal distribution	Wilcoxon Rank Sum (within groups; PPC group - post vs. pre active stimulation)	R	V = 81	p = 0.252		mean = 0.0444, 95% CI [-0.0344 0.1270]
o	3A	Current	DLPFC and Hippocampal-LPOC changes (a priori)	Non-normal distribution	Wilcoxon Rank Sum (within groups; PPC group - DLPFC-LPOC vs. Hippocampal-LPOC FC)	R	V = 75	p = 0.421		mean = 0.0344, 95% CI [-0.0636 0.1593]
p		Current	GC-LPOC changes (a priori)	Non-normal distribution	Wilcoxon Rank Sum (within groups; PPC group - post vs. pre active stimulation)	R	V = 94	p = 0.055		mean = 0.0179, 95% CI [-0.0006 0.0434]
q		Current	GC and Hippocampal-FC changes (a priori)	Non-normal distribution	Wilcoxon Rank Sum (within groups; PPC group - post vs. pre active stimulation)	R	V = 92	p = 0.073		mean = 0.0641, 95% CI [-0.0066 0.1547]
r		Current	DLPFC and Hippocampal Target changes (control analysis)	Normally distributed	Paired T-test (within-groups; PPC group - post vs. pre active stimulation)	R	T(14) = 0.949	p = 0.359		mean = 0.048 95% CI [-0.061 0.157]
S		Current	DLPFC and stimulus location changes (control analysis)	Non-normal distribution	Wilcoxon Rank Sum (within-groups; PPC group - post vs. pre active stimulation)	R	V = 68	p = 0.679		mean = 0.026 95% CI [-0.103 0.121]
t		Current	Changes in PPC GC	Non-normal distribution	Wilcoxon Rank Sum (within-groups; PPC group - post vs. pre active stimulation)	R	V = 92	p = 0.073		mean = 0.022 95% CI [-0.005 0.050]
u	3B	Current	Hippocampal FC changes within Yeo	Normally distributed	Paired T-test (within groups; PPC group - post vs. pre active)	R	T(16) = 10.96	p = 7.6 x 10 ⁻⁹		mean = 0.0900, 95% CI [0.0725 0.1073]

			Networks		stimulation)					
v	3B	Wang et al. (2014)	Hippocampal FC changes within Yeo Networks	Normally distributed	Paired T-test (within groups; PPC group - post vs. pre active stimulation)		R	T(16) = 11.27	$p = 5.10 \times 10^{-9}$	mean = 0.0169, 95% CI [0.0138 0.0201]
w	3B	Both samples	Hippocampal FC changes within Yeo Networks	Normally distributed	Paired T-test (between groups; Current vs. Wang - active stimulation)		R	T(32) = 8.75	$p = 5.42 \times 10^{-10}$	95% CI [0.0560 0.0900]
x	6	Both samples	Hippocampal FC changes within Yeo Networks	Non-Normally distributed	Spearman correlation across samples (Current and Wang)		R	$r = 0.51$	$p = 0.037$	95% CI [0.0389 0.7956]
y		Both samples	GC changes within Yeo Networks	Non-Normally distributed	Spearman correlation across samples (Current and Wang)		R	$r = 0.16$	$p = 0.536$	95% CI [-0.3419 0.5989]
z	8	Current	Hippocampal FC changes in significant regions ($p < 0.01$)	Non-normal distribution	Spearman correlation (within groups; Baseline Hippocampal FC and Hippocampal-FC Changes)		R	$r = 0.39$	$p = 1.0 \times 10^{-4}$	95% CI [0.2002 0.5453]
aa		Current	Hippocampal FC changes in significant regions ($p < 0.01$) - outlier removed	Normally distributed	Pearson correlation (within groups; Baseline Hippocampal FC and Hippocampal-FC Changes)		R	$r(92) = 0.47$	$p = 1.14 \times 10^{-6}$	95% CI [0.2955 0.6141]
bb	8	Current	GC changes in significant regions ($p < 0.01$)	Non-normal distribution	Spearman correlation (within groups; Baseline GC and GC Changes)		R	$r = -0.08$	$p = 0.39$	95% CI [-0.2593 0.1046]